Charge-to-Spin Conversion and Spin Diffusion in Bi/Ag Bilayers Observed by Spin-Polarized Positron Beam

H. J. Zhang,[1,*] S. Yamamoto,[2] B. Gu,[3] H. Li,[1] M. Maekawa,[1] Y. Fukaya,[1] and A. Kawasuso[1]
[1]Advanced Science Research Center, Japan Atomic Energy Agency, 1233 Watanuki, Takasaki, Gunma 370-1292, Japan
[2]Quantum Beam Science Directorate, Japan Atomic Energy Agency, 1233 Watanuki, Takasaki, Gunma 370-1292, Japan
[3]Advanced Science Research Center, Japan Atomic Energy Agency, 2-4 Shirakata Shirane, Tokai-mura, Ibaraki 319-1195, Japan
(Received 22 January 2015; revised manuscript received 12 March 2015; published 22 April 2015)

Charge-to-spin conversion induced by the Rashba-Edelstein effect was directly observed for the first time in samples with no magnetic layer. A spin-polarized positron beam was used to probe the spin polarization of the outermost surface electrons of $Bi/Ag/Al_2O_3$ and $Ag/Bi/Al_2O_3$ when charge currents were only associated with the Ag layers. An opposite surface spin polarization was found between $Bi/Ag/Al_2O_3$ and $Ag/Bi/Al_2O_3$ samples with the application of a charge current in the same direction. The surface spin polarizations of both systems decreased exponentially with the outermost layer thickness, suggesting the occurrence of spin diffusion from the Bi/Ag interface to the outermost surfaces. This work provides a new technique to measure spin diffusion length.

DOI: 10.1103/PhysRevLett.114.166602 PACS numbers: 72.25.Ba, 71.70.Ej, 73.20.At, 78.70.Bj

In the last few years, increased attention has been paid to spintronics due to its potential industrial applications to data processing and information storage. The charge-to-spin conversion in nonmagnetic materials, a central issue in spintronics, is usually realized via the spin Hall effect (SHE), the Rashba-Edelstein effect (REE), and topological insulators [1].

The REE is the energy splitting of spin bands induced by spin-orbit coupling and broken spatial symmetry. In a two-dimensional (2D) electron gas system, the REE Hamiltonian is usually expressed as $H_R = \alpha_R(k \times \hat{z}) \cdot \sigma$, where α_R is the Rashba parameter, k is the electron momentum, $\hat{z}$ is the unit vector of surface normal, and σ is the vector of the Pauli matrix [2]. Giant REE has been found in Bi/Ag, Pd/Ag, and Sb/Ag surface alloy systems by using angle-resolved photoemission spectroscopy [3–5]. Recently, Rojas Sánchez *et al.* reported the spin-to-charge conversion due to the giant REE at the Bi/Ag interface [6]. They used microwave spin pumping to inject a spin current from a NiFe layer into a Bi/Ag bilayer and detected the resulting charge current. They proposed that the spin-to-charge conversion could be ascribed to the REE coupling at the Bi/Ag interface but not the SHE. Their findings imply that the REE is more efficient than the SHE to produce spin-to-charge conversion in spintronics. It is anticipated that the charge-to-spin conversion is also possible due to the giant REE at the Bi/Ag interface.

Positronium (Ps), which is the bound state of a positron and an electron, can only be formed at a local region where the electron density is low enough (typically, less than 10^{13} cm^{-2} in 2D density) [7]. Therefore, in a metal, formation of Ps is only possible at the outermost surface (vacuum side, a few Å away from the first surface layer [8]). There are two types of Ps: ortho-Ps (spin triplet, $|S, m\rangle = |1, 1\rangle$, $|1, -1\rangle$, and $|1, 0\rangle$) and para-Ps (spin singlet, $|S, m\rangle = |0, 0\rangle$). Para-Ps decays into two γ rays with energy of ~511 keV, and is difficult to distinguish from free positron-electron two-γ annihilation. In contrast, ortho-Ps, which decays mostly into three γ rays (the decay possibilities into other odd numbers of γ rays are negligibly small) with energy ranging between 0 and 511 keV, is distinguishable from two-γ events. Inspired by the exciting progress of spintronics in the last decade, a spin-polarized positron beam was developed in order to detect the spin polarization of the outermost surface electrons [9,10].

The change in the ortho-Ps annihilation intensity is obtained by integrating the intensity over part of the energy spectrum that is below 511 keV: $R = A_L/A_P$, where A_L is the area under the energy curve in the low energy region (from 383 to 468 keV), and A_P is the area under the 2γ peak (from 494 to 528 keV). When the Ps formation probability is low, the increment of R from R_0 (subscript "0" means no Ps formation) is proportional to the ortho-Ps intensity ($F_{\mathrm{Ps}}^{3\gamma}$),

$$\Delta R = R - R_0 \propto F_{\mathrm{Ps}}^{3\gamma}. \tag{1}$$

In this study, R and R_0 were measured using positron implantation energies of $E_+ = 50$ eV and 12 keV, respectively.

The asymmetry of ΔR that is induced by the spin flip of the outermost electrons ($+P_- \leftrightarrow -P_-$) can be written as [11]

$$\frac{\Delta R(+P_-) - \Delta R(-P_-)}{\Delta R(+P_-) + \Delta R(-P_-)} = \frac{2\epsilon(1) - \epsilon(0)}{2\epsilon(1) + \epsilon(0)} P_+ P_-^y, \tag{2}$$

where $\epsilon(1)$ and $\epsilon(0)$ are the detection efficiencies of annihilation γ rays from $|1, 1\rangle$ plus $|1, -1\rangle$ and $|1, 0\rangle$,

respectively. From the known values of P_+, ϵ, and the experimental asymmetry, the transverse spin polarization (P_-^y) can be determined. For our detector alignment (perpendicular to the positron beam), the factor $[2\epsilon(1)-\epsilon(0)]/[2\epsilon(1)+\epsilon(0)]$ equates to a constant of 0.6.

A schematic of the spin-polarized Ps annihilation experiment is shown in Fig. 1(a). A transversely spin-polarized positron beam was generated by a ^{22}Na source (~370 MBq) and an electrostatic beam apparatus. The base pressure of the positron beam apparatus was $\sim 6\times 10^{-8}$ Pa. The final beam diameter was 1 mm. The spin polarization of the positron beam, P_+, was measured to be 0.3 [12]. The beam was guided to inject into the center of a sample. A reversible direct current ($\pm j_c$), which was perpendicular to P_+, was applied to the two sample ends through two electrodes. The beam energy E_+ was adjusted to 50 eV by a deceleration tube from the initial value of 12 keV. The center of the sample was electrically grounded. The Ps annihilation γ rays were detected by using a high-purity Ge detector.

The component of the surface spin polarization (P_-) along the y axis was obtained from

$$P_-^y = P_- \cos\phi = \frac{\Delta R_{+j_c} - \Delta R_{-j_c}}{0.18(\Delta R_{+j_c} + \Delta R_{-j_c})}, \qquad (3)$$

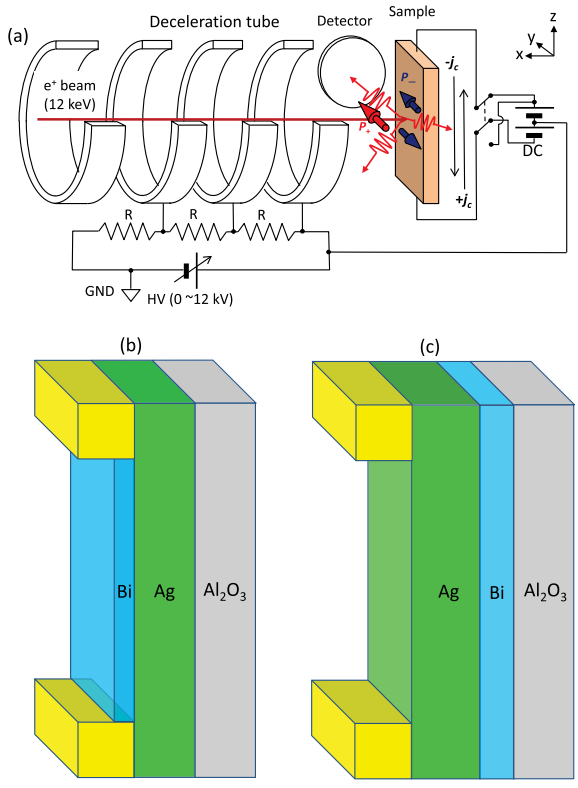

FIG. 1 (color online). The positron beam and the samples. (a) Schematic of the spin-polarized positron beam. The sample layer stack of (b) Bi/Ag(25)/Al_2O_3 and (c) Ag/Bi(8)/Al_2O_3. The yellow blocks represent the Mo electrodes.

where ϕ is the relative angle of P_- to P_+ (y axis), ΔR_{+j_c} and ΔR_{-j_c} are the three-γ annihilation intensities that correspond to an input charge current density of $+j_c$ and $-j_c$, respectively. In this experiment, the charge current was repeatedly reversed between $+j_c$ and $-j_c$. To determine P_-^y, the averages of all ΔR_{+j_c} and ΔR_{-j_c} were calculated. The positive (negative) sign of P_-^y corresponds to the direction of surface spin polarization in the y axis ($-y$ axis) with an input charge current of $+j_c$ in the z direction.

Two types of Bi/Ag bilayer structures, Bi(0–5)/Ag(25)/Al_2O_3 and Ag(25–500)/Bi(8)/Al_2O_3 (numbers in round parenthesis denote film thickness in nm), were prepared on α-Al_2O_3[0001] substrates. As shown in Figs. 1(b) and 1(c), both samples have the Ag layer connected to the two electrodes of the dc power supply. To determine the resistivity of Bi films, three Bi films (100, 200, and 500 nm) were deposited on α-Al_2O_3[0001] substrates [13]. Consequently, the resistivity of the present Bi films was determined to be ~300 $\mu\Omega$ cm, which was approximately 60 times larger than that of Ag films (~5 $\mu\Omega$ cm). Thus, the charge currents mainly flow in the Ag layers.

The square-shaped substrates with length of 20 mm and width of 5–7 mm, were cut from α-Al_2O_3[0001] wafers (mean roughness <0.1 nm). All film depositions were carried out at a substrate temperature of 300 K. The substrates were annealed at 873 K for 30 min in a vacuum chamber (with a base pressure of 3×10^{-7} Pa), which was separated from the beam apparatus. The preparation of each Ag/Bi/Al_2O_3 sample was completed in this chamber. First, the Bi layer was deposited onto the substrate by thermal deposition with Bi granules (99.9999%). Subsequently, using rf magnetron sputtering with an Ag target (99.99%), the Ag layer was deposited onto the Bi layer in a pure Ar (99.999%) ambient at a pressure of 0.3 Pa. The growth rates of Bi and Ag in this chamber were 0.1 and 1.9 nm/min, respectively. During the Bi deposition process, the Bi thickness was monitored by using a quartz crystal thickness monitor (SQM-160, Sigma instruments, measurement error of ±0.1 nm) that was positioned close to the substrate. The Ag/Bi/Al_2O_3 sample was then transferred to another chamber that was connected to the beam apparatus. The transfer took place through air and took approximately 20 minutes. To remove any oxide layer from the sample surface, a 1 keV Ar^+ sputtering was utilized.

Each Bi/Ag/Al_2O_3 sample was prepared as follows: The Ag film was deposited onto the substrate in the above separated chamber. Subsequently, the Ag/Al_2O_3 sample was transferred to the chamber that was connected to the beam apparatus through air within 20 minutes. After cleaning the Ag surface with a 1 keV Ar^+ sputtering, the Bi film was deposited at a growth rate of ~0.05 nm/min.

The crystallinity and surface roughness of samples were characterized by XRD patterns (SmartLab, Rigaku) and atomic force microscopy (AFM) observation (AFM5300E,

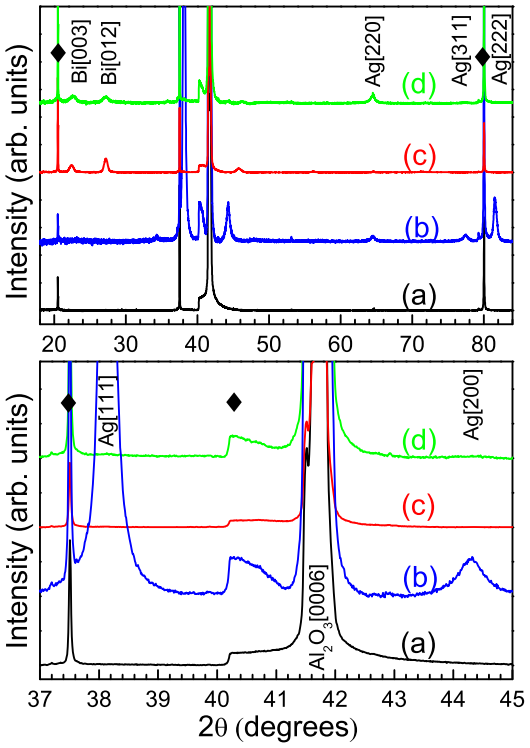

FIG. 2 (color online). XRD patterns of (a) α-Al_2O_3 substrate, (b) $Ag(25)/Al_2O_3$, (c) $Bi(8)/Al_2O_3$, and (d) $Ag(25)/Bi(8)/Al_2O_3$. The "filled diamond" marks represent the imperfections in the α-Al_2O_3 substrates.

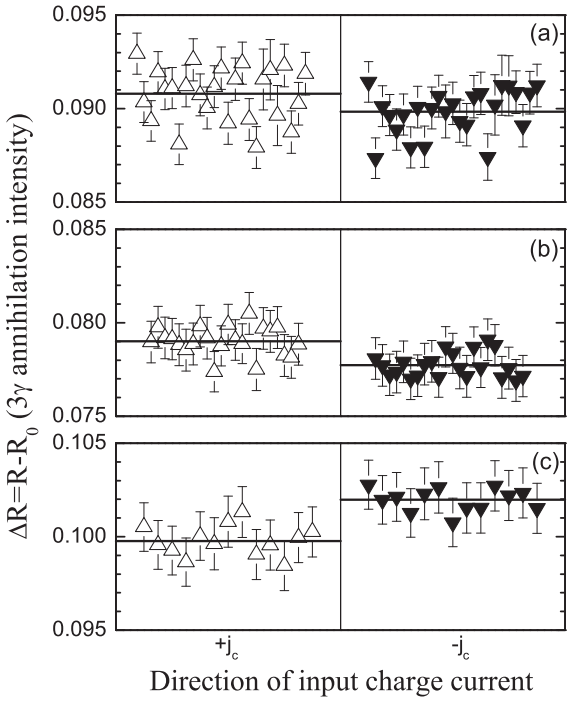

FIG. 3. Variation of ΔR as a function of input charge current of $+j_c$ and $-j_c$ for (a) $Ag(25)/Al_2O_3$ at $j_c = 89.3$ A/m, (b) $Bi(0.3)/Ag(25)/Al_2O_3$ at $j_c = 18.9$ A/m, and (c) $Ag(25)/Bi(8)/Al_2O_3$ at $j_c = 17.5$ A/m.

Hitachi). Figure 2 shows the XRD $\theta - 2\theta$ curves: The Ag film in the $Ag(25)/Al_2O_3$ sample is a polycrystal with the (111), (200), (220), and (311) planes. The Bi layer of the $Ag(25)/Bi(8)/Al_2O_3$ is also polycrystalline with the (012) and (003) planes. The Ag layer of the $Ag(25)/Bi(8)/Al_2O_3$ exists mainly in the (220) orientation [14]. From AFM images, the mean roughnesses of $Ag(25)/Al_2O_3$ and $Bi(8)/Al_2O_3$ were determined to be approximately 1.1 and 2.5 nm, respectively. Additionally, the mean grain diameters of Ag in $Ag(25)/Al_2O_3$ and Bi in $Bi(8)/Al_2O_3$ were found to be ~40 nm from AFM measurements.

Various thicknesses of Bi layers ($d_{Bi} = 0.1$, 0.2, 0.3, 0.6, 1, 2, 3, and 5 nm) were deposited on $Ag(25)/Al_2O_3$. The same charge current of 0.1 A (corresponding to the 2D current density of $j_c = 14$–19 A/m) was applied. For the $Ag(25)/Al_2O_3$ sample, the difference of $\Delta R_{\pm j_c}$ was rather small at $j_c \sim 15$ A/m and could only be observed at much higher j_c. Figure 3(a) shows $\Delta R_{\pm j_c}$ for $Ag(25)/Al_2O_3$ at $j_c = 89.3$ A/m. The surface spin polarization of 3.2% that is estimated from Fig. 3(a), which corresponds to 0.5% at $j_c = 15$ A/m, is probably induced by the spin Hall effect in Ag film. Figure 3(b) shows that the difference of $\Delta R_{\pm j_c}$ of $Bi(0.3)/Ag(25)/Al_2O_3$ is larger than that of the $Ag(25)/Al_2O_3$ sample, even though j_c is much lower.

Figure 4 shows the Bi thickness dependence of the surface spin polarizations that normalized to the values at $j_c = 15$ A/m. The surface spin polarization increases from 0.5 to 0.9% with increasing d_{Bi} from 0 to 0.2 nm, reaches 4.1% at $d_{Bi} = 0.3$ nm, and subsequently decreases gradually for $d_{Bi} > 0.3$ nm. Considering the Bi atomic radius (0.15 nm), $d_{Bi} = 0.3$ nm is approximately one monolayer. As shown by the solid line in Fig. 4, the above Bi thickness dependence of the surface spin polarization can be fitted by an exponential function:

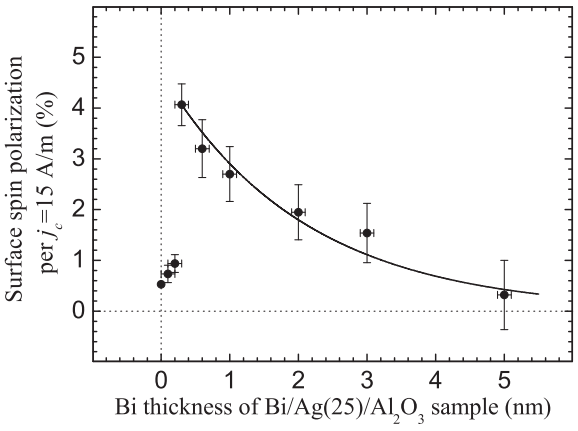

FIG. 4. The surface spin polarization of $Bi/Ag(25)/Al_2O_3$ samples as a function of Bi thickness. The six data points of $Bi(\geq 0.3)/Ag(25)/Al_2O_3$ were fitted to an exponential function of Eq. (4).

$$P^{y}_{-}(d_{\mathrm{Bi}}) = P^{y}_{-}(0.3)\exp[-0.48(d_{\mathrm{Bi}} - 0.3)]. \quad (4)$$

Similarly to the $\mathrm{Bi/Ag(25)/Al_2O_3}$ samples, Ag layers of different thicknesses ($d_{\mathrm{Ag}} = 25$, 100, 200, 300, 400, 500 nm) were deposited on $\mathrm{Bi(8)/Al_2O_3}$. The input charge current was also regulated to 0.1 A for each sample, and the surface spin polarization was normalized to the value at $j_c = 15$ A/m. As shown in Fig. 3(c), the difference of $\Delta R_{\pm j_c}$ is observed at $d_{\mathrm{Ag}} = 25$ nm. More importantly, its magnitude and sign are comparable and opposite, respectively, to those of $\mathrm{Ag(25)/Al_2O_3}$ and $\mathrm{Bi/Ag(25)/Al_2O_3}$. The opposite sign indicates an opposite surface spin polarization. Figure 5 shows that the surface spin polarization decreases with increasing d_{Ag}. Again, this can be fitted by an exponential function:

$$P^{y}_{-}(d_{\mathrm{Ag}}) = P^{y}_{-}(25)\exp[-0.0028(d_{\mathrm{Ag}} - 25)]. \quad (5)$$

The observed opposite sign in the surface spin polarization and the thickness dependencies for $\mathrm{Bi/Ag(25)/Al_2O_3}$ and $\mathrm{Ag/Bi(8)/Al_2O_3}$ suggest that excess electron spins generated at the Bi/Ag interface diffuse into both Bi and Ag layers and eventually appear at the outermost surfaces. Also, the current-induced spin polarization within the Ag layers of $\mathrm{Ag/Bi(8)/Al_2O_3}$ samples is overcompensated by excess and opposite spins supplied from the Bi/Ag interface.

We assume a simple exponential form of $\exp(-d/\lambda_{sd})$ for spin diffusion, where λ_{sd} is the spin diffusion length and the prefactors in the exponentials of Eqs. (4) and (5) correspond to $1/\lambda_{sd}$. Thus, we determine a spin diffusion length of $\lambda_{sd}(\mathrm{Bi}) = 1/0.48 \cong 2.1$ nm for the Bi layer and $\lambda_{sd}(\mathrm{Ag}) = 1/0.0028 \cong 357$ nm for the Ag layer. The spin diffusion length in Bi is comparable to a recent value of $\lambda_{sd}(\mathrm{Bi}) = 1.2$ nm that was obtained from the inverse SHE of a Py/Bi bilayer [15]. Also, the above $\lambda_{sd}(\mathrm{Ag})$ of 357 nm does not conflict with the previous reports of 132, 152, 700, and 300 nm [16–18].

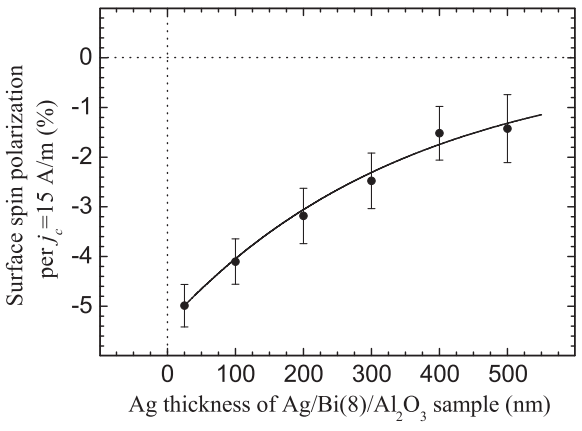

FIG. 5. The surface spin polarization of $\mathrm{Ag/Bi(8)/Al_2O_3}$ samples as a function of Ag thickness. The data were fitted to an exponential function of Eq. (5).

The spin diffusion length is a critical parameter in spintronics. The present study demonstrates that it has the potential to quantitatively characterize the spin diffusion length by detecting the surface spin polarization of samples with different thicknesses of material upon the same film with a known value of spin polarization [such as $\mathrm{Ag(25)/Bi(8)/Al_2O_3}$].

In the study of spin-to-charge conversion in Bi/Ag bilayers, the authors attributed the spin-to-charge conversion to the inverse REE but not the inverse SHE since the spin Hall angle of a BiAg alloy (−2.3%) has the opposite sign to their observation [19]. Considering the fact that the above-obtained spin diffusion lengths agree with those reported so far, the spin polarizations on the outermost surfaces of the Bi/Ag system observed here may be a consequence of the REE, which is the inverse mechanism of the one observed by Rojas Sánchez *et al.* with the spin pumping method.

The charge-to-spin conversion in a sample that contains a magnetic layer has been observed before. In 2010, Miron *et al.* detected a current-driven spin torque induced by the REE in $\mathrm{Pt(3)/Co(0.6)/Al(1.6)/SiO_2}$ [20]. In 2011, they observed the perpendicular switching of a single Co ferromagnetic layer in the same sample [21]. Our previous report on current-induced spin polarization of six transition metals (Pt, Pd, Au, Cu, Ta, and W) was tentatively explained as the surface spin accumulation due to the REE [10]. These samples were also associated with the magnetic layer due to the ferromagnetic property of the nanoscaled Pt and Pd. The validity of the explanation still remains a problem that needs to be experimentally addressed. In this sense, the present observation of opposite spin polarizations at opposite surfaces in Bi/Ag bilayers, as far as we know, is the first direct observation of the REE in a sample with no magnetic layer inside.

The spin density $\langle \delta s \rangle$ resulting from the REE and a charge current is given by [22]

$$\langle \delta s \rangle = \frac{m_e^* \alpha_R}{e\hbar \mathcal{E}_F} j_c, \quad (6)$$

where m_e^* is the effective electron mass, e is the elementary charge, and $\mathcal{E}_F$ is the Fermi energy. For the Bi/Ag[111] system, $m_e^* = 0.35\ m_0$ (m_0 is the electron rest mass), $\alpha_R = 3.05 \times 10^{-10}$ eVm, and $\mathcal{E}_F = 0.18$ eV is calculated from the Fermi wavelength $k_F = 0.13$ Å^{-1} and m_e^* [3]. Thus, at the Bi/Ag interface, $\langle \delta s \rangle \approx 5 \times 10^{10}$ cm^{-2} for $j_c = 15$ A/m. On a metal surface, Ps is formed at the vacuum side where the electron density (n_{2D}) is low enough, typically, less than 10^{13} cm^{-2}. For the Bi surface, $n_{2D} = (0.5 \sim 4) \times 10^{13}$ cm^{-2} at the first surface layer [23–25], which may nearly fulfill the above Ps formation condition. For the Ag surface, such a low electron density is available at a vacuum region, a few Å away from the first surface layer [8]. Therefore, an observable spin polarization

P_{-}^{y} is estimated to be at least (0.1–1)%. Thus, the order of magnitude of the spin polarization observed here, $P_{-}^{y} = (4–5)\%$, could be explained by the REE.

In conclusion, we demonstrate charge-to-spin conversion in Bi/Ag bilayers by using spin-polarized Ps annihilation spectroscopy. Direct evidence of spin diffusion is found by analyzing the outermost layer thickness dependence of surface spin polarization of $Bi/Ag/Al_2O_3$ and $Ag/Bi/Al_2O_3$ samples.

We are grateful to J. Ieda and S. Maekawa of JAEA, T. Seki, K. Takanashi, and E. Saitoh of Tohoku University for their valuable suggestions and discussions. This work was financially supported by JSPS KAKENHI under Grant No. 24310072 and the NSFC under Grant No. 11475130.

*zhang.hongjun@jaea.go.jp

[1] S. Maekawa, S. O. Valenzuela, E. Saitoh, and T. Kimura, *Spin Current* (Oxford University Press, Oxford, 2012).
[2] Y. A. Bychkov and E. I. Rashba, J. Phys. C **17**, 6039 (1984).
[3] C. R. Ast, J. Henk, A. Ernst, L. Moreschini, M. C. Falub, D. Pacilé, P. Bruno, K. Kern, and M. Grioni, Phys. Rev. Lett. **98**, 186807 (2007).
[4] C. R. Ast, G. Wittich, P. Wahl, R. Vogelgesang, D. Pacilé, M. C. Falub, L. Moreschini, M. Papagno, M. Grioni, and K. Kern, Phys. Rev. B **75**, 201401 (2007).
[5] L. Moreschini, A. Bendounan, I. Gierz, C. R. Ast, H. Mirhosseini, H. Höchst, K. Kern, J. Henk, A. Ernst, S. Ostanin *et al.*, Phys. Rev. B **79**, 075424 (2009).
[6] J. C. Rojas Sánchez, L. Vila, G. Desfonds, S. Gambarelli, J. P. Attané, J. M. De Teresa, C. Magén, and A. Fert, Nat. Commun. **4**, 2944 (2013).
[7] A. Held and S. Kahana, Can. J. Phys. **42**, 1908 (1964).
[8] N. D. Lang and W. Kohn, Phys. Rev. B **1**, 4555 (1970).
[9] A. Kawasuso, Y. Fukaya, M. Maekawa, H. J. Zhang, T. Seki, T. Yoshino, E. Saitoh, and K. Takanashi, J. Magn. Magn. Mater. **342**, 139 (2013).
[10] H. J. Zhang, S. Yamamoto, Y. Fukaya, M. Maekawa, H. Li, A. Kawasuso, T. Seki, E. Saitoh, and K. Takanashi, Sci. Rep. **4**, 4844 (2014).
[11] D. W. Gidley, A. R. Köymen, and T. W. Capehart, Phys. Rev. Lett. **49**, 1779 (1982).
[12] A. Kawasuso and M. Maekawa, Appl. Surf. Sci. **255**, 108 (2008).
[13] C. Yang, Research Project (on the Internet) in Research Experiences for Undergraduates, Materials Physics, Florida University, 2008 (unpublished).
[14] M. A. Majeed Khan, S. Kumar, M. Ahamed, S. A. Alrokayan, and M. S. AlSalhi, Nanoscale Res. Lett. **6**, 434 (2011).
[15] D. Hou, Z. Qiu, K. Harii, Y. Kajiwara, K. Uchida, Y. Fujikawa, H. Nakayama, T. Yoshino, T. An, K. Ando *et al.*, Appl. Phys. Lett. **101**, 042403 (2012).
[16] R. Godfrey and M. Johnson, Phys. Rev. Lett. **96**, 136601 (2006).
[17] T. Kimura and Y. Otani, Phys. Rev. Lett. **99**, 196604 (2007).
[18] Y. Fukuma, L. Wang, H. Idzuchi, S. Takahashi, S. Maekawa, and Y. Otani, Nat. Mater. **10**, 527 (2011).
[19] Y. Niimi, H. Suzuki, Y. Kawanishi, Y. Omori, T. Valet, A. Fert, and Y. Otani, Phys. Rev. B **89**, 054401 (2014).
[20] I. M. Miron, G. Gaudin, S. Auffret, B. Rodmacq, A. Schuhl, S. Pizzini, J. Vogel, and P. Gambardella, Nat. Mater. **9**, 230 (2010).
[21] I. M. Miron, K. Garello, G. Gaudin, P.-J. Zermatten, M. V. Costache, S. Auffret, S. Bandiera, B. Rodmacq, A. Schuhl, and P. Gambardella, Nature (London) **476**, 189 (2011).
[22] P. Gambardella and I. M. Miron, Phil. Trans. R. Soc. A **369**, 3175 (2011).
[23] C. R. Ast and H. Höchst, Phys. Rev. Lett. **87**, 177602 (2001).
[24] T. Hirahara, I. Matsuda, S. Yamazaki, N. Miyata, S. Hasegawa, and T. Nagao, Appl. Phys. Lett. **91**, 202106 (2007).
[25] N. Marcano, S. Sangiao, C. Magen, L. Morellon, M. R. Ibarra, M. Plaza, L. Perez, and J. M. De Teresa, Phys. Rev. B **82**, 125326 (2010).